The second virial coefficient of hard alkane models

L. G. MacDowell and C. Vega
Departamento de Quimica Fisica, Facultad de Ciencias Quimicas, Universidad Complutense, 28040 Madrid, Spain

(Received 28 January 1998; accepted 23 June 1998)

The second virial coefficient for hard models of alkanes and other flexible molecules is determined numerically using a new algorithm which increases the speed of the calculations by a few orders of magnitude. For alkanes with few carbon atoms, linear and branched chains were considered and the effect of branching was analyzed. For linear hard alkanes, the second virial coefficient was computed for chains with up to 600 carbon atoms and the scaling behavior was studied. The effect of changes in the chemical structure of a flexible molecule (i.e., bond length, bond angle) was also studied. A fast and efficient empirical methodology to estimate the second virial coefficient of hard chains is given. This methodology uses ideas of convex body geometry. It is shown that the proposed methodology yields very good estimates of the second virial coefficient for chains with up to 100 monomer units, but it predicts incorrectly the scaling law. The virial coefficients provided in this work can be useful in the search of an equation of state for hard alkanes, since it is likely that a good equation of state should provide good estimates of the second virial coefficient. © *1998 American Institute of Physics.* [S0021-9606(98)50237-1]

I. INTRODUCTION

In the last 15 years, the interest of the statistical thermodynamics community on flexible molecules has increased considerably. Now, a number of simulation and theoretical studies are available for these molecules.[1–14] It is likely that perturbation theories will play a fundamental role in improving our understanding of the behavior of melts and polymer solutions. To develop these perturbation theories, one needs a good equation of state for the hard flexible model. At this point, there is a relatively good understanding of the behavior of some flexible models, such as the pearl-necklace model (a collection of flexible tangent hard spheres). For this model, second virial coefficients,[15] simulation data[6,10] and good theoretical equations of state (EOS) are available.[10,12–14] However, the situation is not so satisfactory for hard models of somewhat more realistic polymers as for instance the alkane series. Recently, we have presented simulation results for the EOS of repulsive *n*-alkanes with up to 30 carbon atoms,[16,17] as well as a methodology to estimate the second virial coefficient.[17] In addition to the interest that the second virial coefficient of chains have per se, we found that a very good EOS could be obtained for hard *n*-alkanes, by forcing Wertheim's equation for tangent hard spheres[12,13] to reproduce the estimate of the second virial coefficient as obtained from our procedure. In this way, we have proposed what we believe is the first reliable EOS for hard *n*-alkanes.[17] However, the situation is not fully satisfactory in several respects. First, we do not know if our estimates of the second virial coefficient of hard *n*-alkanes are in good agreement with the exact values. Second, very little is known on the second virial coefficient of long hard models, describing approximately the shape of a real polymer such as polyethylene. Finally, it is also interesting to analyze the role of branching on the second virial coefficient, especially for short flexible molecules.

In this work, we try to clarify some of these issues. First, we shall compute numerically the second virial coefficient of hard *n*-alkanes with up to 600 carbon atoms. In this way, it will be possible to determine if the methodology proposed in our previous work is indeed reliable.[17] These data can also be useful for other workers looking for good EOS of hard models of polyethylene, since one would expect that they should yield a reasonable value of the second virial coefficient. Second, we will test the general applicability of our method by comparing its predictions with the exact virial coefficient of several models. Third, the virial coefficient of branched alkanes will be computed and this will provide ideas on the effect of branching. Finally, we study the scaling behavior of the second virial coefficient of long idealized flexible molecules, with up to 1000 monomers. This study was made possible due to the use of a new algorithm which increases the speed of the numerical calculations of the second virial coefficient by a few orders of magnitude.

The scheme of this paper is as follows. In Sec. II the models used in this work and the computational details are described. In this section, a methodology to estimate the second virial coefficient of hard chains is also provided. In Sec. III, results are presented for the second virial coefficient of several flexible hard models and compared with the predictions from our methodology. In Sec. IV we analyze the data and the scaling law for the second virial coefficient of very long hard flexible chains.

II. MODELS AND CALCULATIONS

A. Models

Two kinds of hard flexible models have been considered in this work. The first one is an extension of that used in previous work,[16–18] where we attempted to mimic qualitatively the shape of linear alkanes within the united atom

approach. Thus, each CH_n group is modeled as a hard sphere of diameter d. The hard spheres are connected through a bond of length l, chosen such that the reduced bond length, $L^*=l/d$, is set to 0.4123. The bond angle θ is fixed to the tetrahedral value, i.e., 109.5 degrees. The torsional degrees of freedom are treated within the rotational isomeric state approximation[19] (RIS), so that each torsional angle may adopt only three possible states: The *trans* (t), $gauche^+$ (g^+), and $gauche^-$ (g^-) states, which correspond to values of 0, 120 and -120 degrees, respectively. In this way, the number of possible conformations of a given alkane is always finite, but it becomes very large as the length of the chain is increased. A schematic representation of the model may be found in Fig. 1 of Ref. 17.

The Hamiltonian of the system is divided into an intra and an intermolecular contribution, so that the total energy is given by:

$$U=U_{\text{intra}}+U_{\text{inter}}. \tag{1}$$

The intermolecular potential between the molecules is given by a site–site hard sphere interaction, while the intramolecular interaction is divided into a short range part and a long range part, following Flory's division.[19] The long range part corresponds to a hard sphere interaction between monomers (i.e., hard spheres) five or more bonds apart. The short range interaction is given by the following expression:

$$U_{\text{intra}}^{\text{short}}=n_g E_1+n_{g^+g^-}(E_2-E_1), \tag{2}$$

where n_g is the number of pairs of carbon atoms three bonds apart which are in a relative configuration of type gauche and $n_{g^+g^-}$ is the number of pairs of carbon atoms four bonds apart whose relative configuration is either a g^+g^- or g^-g^+ sequence. For linear chains, Eq. (1) is equivalent to the procedure introduced by Flory, which has been used in a previous study of the second virial coefficient of n-alkanes with attractive forces.[20] In this work, we shall use Eqs. (1)–(2) for both linear and branched chains, with $E_1=3337.83$ J/mol and $E_2=11711.43$ J/mol.[21] A rigorous description of branched alkanes would involve an individual study of the short range intramolecular interactions for each molecule, but in this work we keep the potential as simple as possible and focus on the effect of branching on the second virial coefficient.

In what follows, this hard alkane model will be denoted as the Flory-like model. It should be noted that the relative populations of the different conformers are temperature dependent through the short range intramolecular interactions, so that B_2 is also temperature dependent. We have thus used a constant temperature of $T=366.88$ K for all the calculations, as in previous work.[16–18]

Additionally, the previous model has been extended to describe what may be considered as the RIS approximation to the well known pearl-necklace model.[6,10] This has been achieved by setting the reduced bond length to one and the short range intramolecular energy parameters to zero ($L^*=1$, $E_1=E_2=0$ J/mol). To keep the number of conformers finite, the bond angle θ has been set to 104.4775 degrees, which is approximately the average angle of tangent hard sphere trimers. Note that, contrary to the Flory-like model, the conformational properties of this pearl-necklace-like model do not depend on temperature.

B. Numerical evaluation of B_2

The second virial coefficient of a flexible molecule is calculated from the average Mayer function according to the following equation:

$$B_2=-2\pi\int_0^\infty \langle f_{ij}(R_{\text{CM}})\rangle_{\text{conf}} R_{\text{CM}}^2 dR_{\text{CM}}, \tag{3}$$

where R_{CM} is the distance between the centers of mass of the molecules, $\langle\rangle_{\text{conf}}$ denotes a weighted conformational average (where the weight is the Boltzmann factor of the intramolecular energy) and the Mayer function for a pair of conformers is given by:

$$f_{ij}(R_{\text{CM}})=\langle \exp(-\beta U_{\text{inter}}^{ij}(R_{\text{CM}},\omega_i,\omega_j))-1\rangle_{\text{ori}}. \tag{4}$$

In this equation, $U_{\text{inter}}^{ij}(R_{\text{CM}},\omega_i,\omega_j)$ is the energy between conformers i and j with relative orientations given by the set of angles ω_i and ω_j, $\langle\rangle_{\text{ori}}$ denotes an unweighted orientational average, and β is defined as $\beta=1/(k_BT)$ where k_B is the Boltzmann constant. For the RIS models, the number of conformers remains finite, so that Eq. (3) may be rewritten as:

$$B_2=\sum_{i=1}^{q}\sum_{j=1}^{q} x_i x_j B_{ij}, \tag{5}$$

where x_i and x_j are the molar fractions of the conformers i and j, respectively, q is the total number of conformers of the molecule and the B_{ij}'s are obtained from integration of f_{ij}. The molar fraction of each conformer is proportional to the Boltzmann factor of the intramolecular energy $\exp(-\beta U_{\text{intra}})$.

For a given relative orientation of a pair of selected conformers, we have evaluated $\exp(-\beta U_{\text{inter}}^{ij}(R_{\text{CM}},\omega_i,\omega_j))$ exactly at 999 points of R_{CM}, ranging from 0 to about five times the mean radius of gyration. This otherwise prohibitively expensive calculation was done by using a new algorithm which requires one single calculation of the interatomic distances for all the points in the R_{CM} segment. Details of this procedure may be found in Appendix A. The orientational averages required to calculate the f_{ij}'s from the intermolecular Boltzmann factor were then evaluated by means of Conroy's multidimensional integration method,[22,23] while the B_{ij}'s were calculated from numerical integration (using Simpson's rule) of the latter function. For molecules with up to eight monomer units, the orientational averages were calculated using 76 079 relative orientations, while 4822 orientations were used for bigger molecules.

The way the conformational average is evaluated depends greatly on the size of the molecules considered. All the conformers of molecules with three or less torsional angles may be enumerated without problems, so that the conformational average was evaluated exactly, by exhaustive enumeration. On the other hand, the number of pairs of different conformers of molecules with more than three torsional angles becomes prohibitively large, so that the average was

evaluated approximately, by randomly selecting pairs of independent conformations, as obtained from a Monte Carlo simulation of the isolated chain. For the virial coefficients of mixtures of butane and long n-alkanes, the conformational population of butane was weighted exactly, while that of the long n-alkanes was weighted by randomly selecting conformers from the MC simulation.

The samples of representative conformers were produced by means of a standard MC algorithm, where trial configurations are accepted or rejected according to the Metropolis criterion.[24] Trial configurations were produced using the pivot algorithm,[25] where an initial configuration is transformed into another by randomly choosing and rotating a torsional angle.

The size of the MC samples ranged from 2000 conformers for chains of 200 or less monomers to 1000 for chains of 400 and 600 monomers, while the number of pairs of conformers chosen to calculate B_2 was roughly equal to the number of conformers of the sample used.

C. Empirical estimation of B_2

In this work we shall also try to estimate the second virial coefficient of hard chains by using convex body geometry[26–28] (CBG). One of the first attempts to introduce CBG ideas in the search for EOS of chains was that of Enciso *et al.*[29] Recently, we have introduced a new methodology[17] which allows to estimate correctly the second virial coefficient of linear chains. Here we shall describe the procedure briefly and we refer the reader to Ref. 17 for further details.

We expect that the virial coefficients of two conformers of the same molecule are not too different, as there are almost no volume differences and the shape is roughly similar. We may then expect that the crossed virial coefficient may be approximately given by the following equation, denoted as Approximation 1:

$$B_{ij}=(B_{ii}+B_{jj})/2. \tag{6}$$

By replacing Eq. (6) into Eq. (5) we obtain:

$$B_2=\sum_{i=1}^{q} x_i B_{ii}. \tag{7}$$

Let us now define the nonsphericity parameter of conformer i, α_i, by the relation:[30]

$$B_{ii}/V_i=1+3\alpha_i, \tag{8}$$

where V_i is the molecular volume of conformer i.

In Ref. 17 we propose a methodology to estimate α_i by using CBG which we shall denote as Approximation 2. According to this methodology, the nonsphericity of a linear chain conformer may be estimated by means of standard convex geometry relations, provided that the mean radius of curvature of the conformer, R_i, is considered as that of an equivalent parallelepiped. This leads to the following equation:

$$\alpha_i=\frac{R_i S_i}{3V_i}+\frac{\left(\frac{L_{tt..t}}{4}+\frac{d}{2}-R_{tt..t}\right)S_{tt..t}}{3V_{tt..t}}, \tag{9}$$

where S_i is the surface of conformer i, R_i is the mean radius of curvature of the equivalent convex body and the second term of the r.h.s. is a correcting term that ensures that the nonsphericity of the all-trans conformer is given almost exactly. The subindex $tt..t$ stands for the all-trans conformer and $L_{tt..t}$ is the distance between the first and the last carbon atom in this configuration.

In order to extend Eq. (9) to branched alkanes we need a prescription for the correction term. The choice we have taken is to define it equal to that of the n-alkane with the same number of carbon atoms (e.g., for 2,3-dimethyl pentane we shall use the correction term for n-heptane).

Finally, by approximating the average of the product of $\alpha_i V_i$ to the product of the separated averages of α_i and V_i (a very good approximation, as the different conformers present different values of α_i but very similar values of V_i), the estimate of the second virial coefficient for the chain, either linear or branched, is given by:

$$B_2=\overline{V}(1+3\overline{\alpha}), \tag{10}$$

where the bar denotes the weighted conformational average. The volume and surface required for the calculation of α_i for a given conformer is evaluated by an exact numerical procedure developed by Dodd and Theodorou.[31] The radius of curvature is evaluated following the procedure described in Ref. 17. The conformational average is then evaluated in a similar manner as that described in the previous section. For molecules with up to five torsional angles, the conformational averages could be calculated exactly by exhaustive enumeration, while those with more than five torsional angles required a MC averaging.

In the next section we present the results of this work.

III. RESULTS

We shall start presenting results for the Flory model.

There are two questions which we would like to answer concerning the second virial coefficient of hard alkanes, namely, (i) how sensitive is it to the conformation of the chain?; and (ii) how sensitive it is to the effect of branching? The first question tries to explain the effect of flexibility, while the second one tries to explore the differences between different isomers. Let us now focus on the first issue. In Ref. 18 the second virial coefficient was evaluated for different conformers of hard n-alkanes. Moreover, the exact values were compared[17] with the approximated values obtained from convex body theory as described in the previous section. The agreement was found to be good. Here, we shall therefore focus on branched alkanes, for which no result has been so far reported.

In Table I, we present the second virial coefficient for different conformers of the molecule of 2-methyl pentane and 2,3,4-trimethyl pentane. These results were obtained by fixing the conformation of the alkane and determining the second virial coefficient between two identical conformers as if they were considered rigid bodies. As it can be seen, the

TABLE I. Second virial coefficient for 2-methyl pentane and 2,3,4 trimethyl pentane conformers in units of d^3. B_2^{exct} is the exact second virial coefficient. B_2^{CBG} is the CBG prediction proposed in this work. B_2^{Ale} is the prediction using the method proposed by Alejandre *et al.* and α_i is the exact nonsphericity parameter of each conformer. The number of carbon atoms three bonds apart which are in a relative configuration of type gauche is denoted as n_g. The conformers are represented by the conformation of the carbon atoms of the main chain.

conformer	n_g	B_2^{exct}	B_2^{CBG}	B_2^{Ale}	α_i
2-methylpentane					
tt	1	10.184	10.089	10.293	1.346
tg^-	2	9.942	9.883	10.062	1.311
g^-g^+	2	9.322	9.281	9.436	1.241
g^+g^+	2	9.832	9.796	9.974	1.293
g^-g^-	3	9.082	9.087	9.218	1.205
2,3,4-trimethylpentane					
tt	4	12.592	12.500	12.859	1.310
tg^+	5	12.964	12.873	13.286	1.335
tg^-	5	12.371	12.315	12.663	1.285
g^+g^+	6	12.290	12.211	12.575	1.277
g^+g^-	6	11.715	11.666	11.969	1.227
g^-g^+	6	12.322	12.247	12.602	1.282

second virial coefficient changes significantly from one conformer to another, usually decreasing with the number of gauche bonds. It is also clear that, as the number of gauche bonds in the molecule increases, the molecule becomes more spherical (i.e., the nonsphericity parameter takes lower values). The convex body method proposed is able to grasp all of this features and the predicted values are in good agreement with the exact ones.

We now focus on the second issue, i.e., the variation of the second virial coefficient with branching. In Table II, we present results of the second virial coefficient for different hard alkanes. By comparing molecules with the same number of carbon atoms, the following conclusions can be obtained:

(1) For alkanes with the same number of carbon atoms, the second virial coefficient decreases when going from the *n*-alkane to the branched alkane. This effect increases as the number of branches increases.
(2) For two branched alkanes which differ only in the location of the branch, the one with the branch closer to the middle of the main chain will present a smaller value of the second virial coefficient (compare for instance 2-methyl pentane and 3-methyl pentane or 2,2 dimethyl pentane and 3,3 dimethyl pentane).
(3) Two methyl groups on a certain carbon provoke a larger reduction than an ethyl group on the same carbon atom (compare for instance 3,3 dimethyl pentane and 3-ethyl pentane).

TABLE II. Second virial coefficients of several branched and linear alkanes in units of d^3. Notation as in Table I. The symbol *S* denotes the spatial configuration of the asymmetric carbon atom.

Alkane	B_2^{exct}	B_2^{CBG}	B_2^{Ale}	$\overline{\alpha}$
n-butane	6.622	6.585	6.658	1.212
2-methyl propane	6.529	6.441	6.571	1.193
n-pentane	8.425	8.348	8.487	1.293
2,2-dimethyl propane	7.993	7.810	8.098	1.218
2-methyl butane	8.115	7.993	8.202	1.239
n-hexane	10.392	10.385	10.474	1.377
2,2-dimethyl butane	9.500	9.402	9.672	1.245
2,3-dimethyl butane	9.593	9.492	9.751	1.259
2-methyl pentane	10.062	9.986	10.181	1.328
3-methyl pentane	9.806	9.751	9.944	1.291
n-heptane	12.531	12.505	12.614	1.464
2,2,3-trimethyl butane	10.910	10.763	11.174	1.255
2,2-dimethyl pentane	11.609	11.438	11.812	1.346
3,3-dimethyl pentane	11.072	10.976	11.324	1.275
3-ethyl pentane	11.528	11.439	11.727	1.335
n-octane	14.806	14.892	14.909	1.548
2,2,3,3-tetramethyl butane	12.198	12.098	12.588	1.249
2,2,3-trimethyl pentane(S)	12.791	12.685	13.117	1.318
2,3,3-trimethyl pentane	12.536	12.475	12.889	1.288
3-ethyl,3-methyl pentane	12.677	12.662	13.024	1.304
2,3,4-trimethyl pentane	12.884	12.794	13.198	1.329

TABLE III. Second virial coefficients in units of the average molecular volume for several models and monomer lengths. The numbers in parenthesis are a measure of the uncertainty as measured by the standard deviation of the calculations. $\overline{V}$, is the average molecular volume in units of d^3, $\overline{\alpha}$ is the average of the nonsphericity parameter. Rest of the notation as in Table I.

N	$\overline{V}$	$B_2^{\text{exct}}/\overline{V}$	$B_2^{\text{CBG}}/\overline{V}$	$B_2^{\text{Ale}}/\overline{V}$	$\overline{\alpha}$
Flory model					
10	3.2204(2)	6.151(4)	6.244(2)	6.190(1)	1.717
30	9.1954(2)	10.98(2)	11.56(1)	10.44(2)	3.302
60	18.1595(7)	16.93(7)	18.0(6)	15.3(4)	5.31
100	30.1101(8)	24.1(6)	24.8(6)	20.6(4)	7.71
200	59.9890(3)	39.54(2)	37.8(1)	30.8(16)	12.85
400	119.7490(2)	65.6(1)	57.4(3)	46.6(4)	21.60
600	179.5060(4)	89.43(2)	72.9(2)	59.2(20)	29.50
Open model					
10	3.2639(1)	6.535(2)	6.666(1)	6.563(2)	1.845
30	9.3512(3)	12.24(4)	13.10(2)	11.68(2)	3.748
60	18.4819(1)	19.90(1)	21.0(3)	17.6(4)	6.298
100	30.6566(1)	29.3(1)	29.6(6)	24.1(8)	9.431
Long model					
10	5.2360	14.42(1)	14.87(3)	14.07(4)	4.474
30	15.7080	33.94(3)	35.38(6)	29.8(4)	10.98
60	31.4159	60.3(1)	58.6(2)	47.3(2)	19.77
100	52.3599	92.2(1)	82.0(3)	65.2(4)	30.42
Pearl-necklace-like model					
10	5.2360	12.55(2)	13.04(6)	12.36(3)	3.85
30	15.7080	24.8(1)	26.3(6)	23.2(4)	7.92
60	31.4159	39.5(1)	41.08(6)	35.08(4)	12.83
100	52.3599	56.7(1)	56.53(6)	47.59(4)	18.61

The results of Table II show clearly the big differences in the second virial coefficient between linear and branched alkanes. For instance, for alkanes with eight carbon atoms, the variations in B_2 can be of up to 20% and differences are expected to be larger for longer chains.

Once more, comparing the numerical values of B_2 with those obtained by using CBG, it can be seen that the agreement is quite good. We have also implemented the methodology proposed by Alejandre *et al.*[32] (which differs from ours in the choice of the equivalent convex body from which the mean radius of curvature is taken). In general, the treatment of this work is somewhat better than the latter method.

We shall analyze now the effect of changing the bond length or bond angle on the second virial coefficient of linear chains. In Table III, results are presented for the Flory model as described in the previous section, for chains with a number of carbon atoms in the range 10–600. We also show, for chains with up to 100 monomers, the results obtained for several modifications of the Flory model, namely, a model with the bond angle increased to 120 degrees (Open model) and a model with the bond length increased to $L^*=1$ (Long Model). Also in Table III we present results for the pearl-necklace-like model described in the previous section. In Table III, the exact and predicted second virial coefficients are shown in units of the molecular volume, so that the results of the different models may be compared without regard to the change in volume.

Inspection of Table III leads to the following conclusions:

(1) The increases of the bond length or bond angle provokes an increase in the value of $B_2/\overline{V}$. In other words, the molecule becomes more anisotropic when increasing either the bond length or bond angle. These trends were anticipated in Ref. 17, based on our methodology to estimate virial coefficients from convex body theory but it is confirmed here by exact numerical determination of the virial coefficients.
(2) The estimates of the second virial coefficient are quite good for all the models, thus showing that the methodology proposed is quite general and can be successfully used for general chain models, regardless of the bond length, angle or torsional energy.

From the results of Tables I–III it is clear that the convex body methodology proposed to estimate the second virial coefficient is reliable. This success is a consequence of two facts. The first is that the second virial coefficients are correctly predicted for the different conformers of a given alkane, as was shown in Table I, while the second is that the approximation represented by Eq. (6) is indeed excellent.

To show that this is so, we present Table IV, where exact results for the crossed coefficients of a few pairs of conformers of C_{200} are compared with those obtained from Approximation 1. The agreement is good, the typical error being of about 1.5%. We also show a comparison between (1) the average of 45 exact crossed virial coefficients, B_{ij}, obtained from a randomly selected sample of 10 conformers, and (2) the average of the corresponding 10 B_{ii}'s, for several

TABLE IV. Test of Approximation 1 for the Flory model. The approximation is tested for a few pairs of conformers of C_{200}. N, number of carbon atoms. B_{ii}^{exct}, exact second virial coefficient for conformer i. B_{ij}^{exct}, exact crossed second virial coefficient for the chosen pair of conformers. B_{ij}^{approx}, estimate of B_{ij} from Eq. (6). % err, mean percent error. We also present results ($N=30,60,100,200$) for the exact average of the 45 different pair of conformers that can be obtained from a random sample of 10 conformers. This average is compared to the value predicted by Eq. (6) (Approximation 1). The second virial coefficients are given in units of d^3.

N	B_{ii}^{exct}	B_{jj}^{exct}	B_{ij}^{exct}	B_{ij}^{approx}	% err
200	2508	2630	2335	2342	0.3
200	1712	2506	2149	2109	1.9
200	1712	2111	1942	1912	1.5
200	2660	1712	2158	2186	1.3
200	2660	2506	2502	2583	3.2
30	-	-	101.8 (5)	102.1 (5)	0.3
60	-	-	305(4)	305(4)	0
100	-	-	729(8)	732(8)	0.01
200	-	-	2235(27)	2230(28)	0.2

chain lengths. As it can be seen, the agreement is quite good. Notice that the error is now smaller (of about 0.2%) than for individual pairs of conformers. This is a consequence of cancellation of errors, as individual B_{ij} are sometimes overestimated whereas other they are underestimated. We can conclude that Eq. (6) is an excellent approximation for estimating the crossed second virial coefficient between two different conformers of the same molecule. Moreover, if one compares the average obtained from the calculation of 10 B_{ii} alone (column labeled as B_{ij}^{approx} in Table IV) with those of the first part of Table III, it can be seen that the average of 10 B_{ii} alone is already a very good estimate of the actual B_2 as calculated from an average of the B_{ij} of 2000 pairs of conformers. This surprising result will be used in the next section to estimate the second virial coefficient of chains with up to 1000 monomers.

We have compared the B_2 obtained for the pearl-necklace-like model (see Table III) with those of the true pearl-necklace model as obtained in Refs. 15, 33. For the true model, one obtains $B_2/V=12.75$, 25.17, 40.23 and 57.81 for $N=10$, 30, 60 and 100, respectively (the results were obtained by interpolation whenever required). As it can be seen, the results for the two models are quite similar. Although this is somewhat expected, it is certainly surprising that both models agree so closely. Recall that the models differ in the fact that the bond angle was fixed in our calculations, whereas the true model is fully flexible (as far as the spheres do not overlap) and that we use the RIS approximation (only three angles are used for each torsional degree of freedom), whereas the true pearl-necklace model can adopt any value of the torsional angle.

Finally, we have evaluated numerically the second virial coefficient for pairs of n-alkanes (as described by the Flory model) of very different length (i.e., C_4+C_{60}, C_4+C_{100}, C_4+C_{200}, and C_4+C_{400}). The results are shown in Table V, along with the predictions obtained from two different methods. The first one is based on an exact equation for the B_2 of two convex bodies, 1 and 2, of different size:[28]

$$B_{12}=\tfrac{1}{2}(V_1+V_2+S_1R_2+S_2R_1). \tag{11}$$

We have used this equation for alkanes of different size, with V, S and R replaced by their mean values and the results are shown in the third column of Table V. The agreement is seen to be reasonable but it deteriorates considerably for large size differences. On the other hand, the following empirical equation is seen to predict the results with an error of less than 5% as it can be seen in Table V:

$$B_{12}=\tfrac{1}{2}\left(B_{11}\frac{V_2}{V_1}+B_{22}\frac{V_1}{V_2}\right). \tag{12}$$

Equation (12) was obtained after an algebraic analysis of Eq. (39) of Ref. 17. In turns out that the approximation given by Eq. (39) of our previous work[17] contains implicitly a prescription for B_{12} of the mixture which is just that given by Eq. (12). Notice that Eq. (12) reduces to Eq. (6) when the two molecules have the same volume as it is almost the case for two conformers of the same chain. The good results of Eq. (12) explain the success of the EOS for mixtures proposed in Ref. 17. Equation (12) is quite successful in predicting the crossed second virial coefficient of chains with large differences in size. However, for true convex bodies with large differences in size (i.e., mixtures of hard spheres) Eq. (12) is poor whereas in this case Eq. (11) is exact.

The results presented so far have illustrated the role of conformation, branching and geometrical parameters (bond length, angle) on the second virial coefficient. Moreover, it has been shown that the methodology proposed previously gives good estimates of the second virial coefficient of chains with up to 100 monomer units, while it reduces the cost of the computations by several orders of magnitude.

TABLE V. Crossed virial coefficients in d^3 units for alkanes (as described by the Flory model) of different length. B_{12}^{exct} is the exact crossed virial coefficient. B_{12}^{CBG} is the estimate given by Eq. (11) and B_{12}^{empi} is the estimate given by Eq. (12).

Mixture	B_{12}^{exct}	B_{12}^{CBG}	B_{12}^{empi}
C_4+C_{60}	53.54(6)	53.90	53.96
C_4+C_{100}	87.0(1)	81.1	86.6
C_4+C_{200}	170.1(2)	154.3	166.5
C_4+C_{400}	336.6(3)	296.6	323.1

TABLE VI. Interpenetration factor ψ for the Flory and for the pearl-necklace-like model. The second and third columns refer to the Flory model, while the rest refers to the pearl-necklace-like model. $\langle S^2\rangle$ is the mean square radius of gyration (in units of d^2) and B_2 is the second virial coefficient in units of d^3.

N	$\langle S^2\rangle$	ψ	B_2	$\langle S^2\rangle$	ψ
100	21.6(1)	0.325(5)	2961(7)	54.7(2)	0.329(3)
200	51.5(4)	0.288(4)	9769(25)	130(1)	0.296(4)
400	120.(2)	0.268(8)	32 480(120)	301(2)	0.279(4)
600	197.(1)	0.261(3)	65 320(240)	489(1)	0.271(2)
800	-	-	108 069(1102)	684(4)	0.271(5)
1000	-	-	163 368(1631)	899(2)	0.272(4)

One obvious question which arises is whether the methodology proposed, based on CBG, correctly predicts the second virial coefficient of polymers (i.e., very long chains). We shall analyze this question in the following section.

IV. THE VIRIAL COEFFICIENT OF VERY LONG CHAINS

The study of the virial coefficient of very long hard chains has interest per se. Experimentally, the osmotic second virial coefficient of polymers under good solvent conditions can be measured and it is thought that it behaves as the second virial coefficient of a hard long chain.[34,35] From a computational point of view, the calculation of the virial coefficient of hard chains presents at the moment some practical difficulties. With the computers now available, the limit in the numerical calculation seems to be located at about 500 monomer units.[33,36–38] Although this is a large number, it is still small compared to the number of monomers of typical polymers (i.e., 1000–1 000 000). Theoretically, de Gennes[39] has developed a model for the scaling of the second virial coefficient of very long chains. Experimental[35] work and recent numerical calculations[15,36,38] seem to confirm de Gennes' ideas. In this section we analyze whether the CBG methods can predict correctly the scaling laws for the second virial coefficient of chains.

In Table III, the second virial coefficient for the Flory model with up to 600 carbon atoms was presented. It can be seen that, although the convex body methodology is quite successful for molecules with up to 100 monomers, it fails for bigger molecules. As it will be shown now, this is due to the fact that the CBG methodology predicts an incorrect scaling.

According to de Gennes, the ratio of the second virial coefficient of the chain divided by the mean squared radius of gyration to the 3/2 power yields a constant in the limit of very long chains. This behavior is usually described in terms of the so-called interpenetration factor, defined by the following ratio:

$$\psi = 2\frac{B_2}{(4\pi\langle S^2\rangle)^{3/2}}, \tag{13}$$

where $\langle S^2\rangle$ is the mean squared radius of gyration.

Evidence that Eq. (13) is correct comes from experimental work and from recent numerical calculations,[15,36,38] as well as from our own results.

In Table VI, we show the $\langle S^2\rangle$ and ψ for the Flory-like model and for the pearl-necklace-like model. Also shown are the B_2 for the latter model for chain lengths of up to 1000 monomers. The B_2 for chains of up to 600 monomers were calculated as explained in Sec. II A, while those of chains of 800 and 1000 monomers were calculated by averaging 250 B_{ii}. As discussed in the previous section we believe that this procedure provides an accurate estimate of the second virial coefficient.

In Fig. 1, ψ is plotted for the Flory- and the pearl-necklace-like model. As can be seen, ψ seems to reach a constant value of 0.26–0.27 for both models, in good agreement with renormalization group theory[40] and with previous numerical work.[36]

According to Eq. (13), B_2 scales as $\langle S^2\rangle^{3/2}$. In good solvent conditions (i.e., for hard intramolecular interactions) it is well known that $\langle S^2\rangle$ scales as:

$$\langle S^2\rangle \propto N^{2\nu}, \tag{14}$$

where N is the number of monomer units. The best estimate of ν now available is 0.588.[41] We checked the scaling law for the mean squared radius of gyration for the chain models of this work and found excellent agreement with Eq. (14) and the value $\nu = 0.588$. Therefore, according to de Gennes, B_2 scales as:

$$B_2 \propto N^{3\nu} \propto N^{1.764}, \tag{15}$$

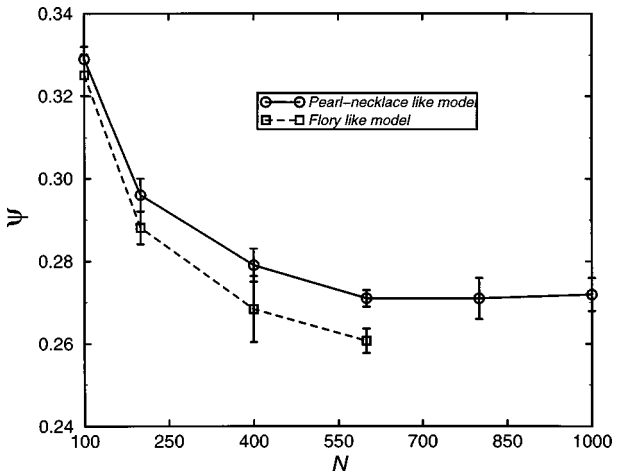

FIG. 1. The interpenetration factor ψ for different values of N and two polymer models. Full line: pearl-necklace-like model; dashed line: Flory model.

and our results support this conclusion (in agreement with previous work by other authors). Which is the scaling law predicted by the convex body treatment? According to this treatment:

$$B_2 = V\left(1 + 3\frac{RS}{3V}\right) \propto RS. \tag{16}$$

Now, both the molecular surface and volume scale as N, whereas the mean radius of curvature as obtained from our methodology scales as the mean radius of gyration (see further discussion of this issue in Appendix B). Therefore, the CBG predicts:

$$B_2 \propto N^{1.588}. \tag{17}$$

Numerical analysis of the scaling law of our estimates of B_2 from the CBG was found to be consistent with Eq. (17). By comparing Eq. (17) with Eq. (15) one concludes that the scaling law predicted by the CBG methodology to estimate B_2 is wrong. When the Alejandre *et al.*[32] recipe is used to predict the mean radius or curvature, the same qualitatively wrong behavior is obtained. In fact, the predicted virial coefficients are low for very long chains, which can be understood by looking at the different scaling laws presented by Eq. (15) (right) and Eq. (17) (wrong). We have also tried to take the mean radius of curvature of the chain from another convex body, as for instance a hard ellipsoid[42] with three different lengths for the main semi-axes, but the results do not improve. In fact, according to Eq. (17), the convex body ideas fail to predict the scaling law of the second virial coefficient of very long chains, regardless of the choice of the convex body from which the mean radius of curvature is taken, since it always leads to a radius of curvature which scales as the mean radius of gyration. However, as described in the previous section, it can be used successfully to predict the virial coefficients of chains with less than 100 monomer units.

Finally, let us discuss briefly the site–site correlation function in the limit of zero density for some of the chains of this work. [The reader is referred to Appendix C (method 1) for details of the calculations.] Let us denote by $\overline{g_{kl}}(r)$ the site–site correlation function between site k of one molecule and site l of another molecule when averaged over all pair of conformers. Although the behavior of the individual $\overline{g_{kl}}(r)$ has some interest, it is obvious that for long chains it is more interesting to discuss the behavior of the site–site correlation function averaged over all pair of sites. This site–site correlation function is defined as:

$$g(r) = \frac{1}{N^2}\sum_{k=1}^{N}\sum_{l=1}^{N}\overline{g_{kl}}(r). \tag{18}$$

In Fig. 2 $g(r)$ is plotted for the pearl-necklace-like model when $N = 10,30,60$. Some obvious features are:

(1) The value of g at contact ($r=\sigma$) decreases with the length of the chain. In fact, it seems to go to zero for very long chains.
(2) The correlation hole [where $g(r)$ is less than 1 by more than 2%] is of the order of three times the mean radius of gyration of the molecule.

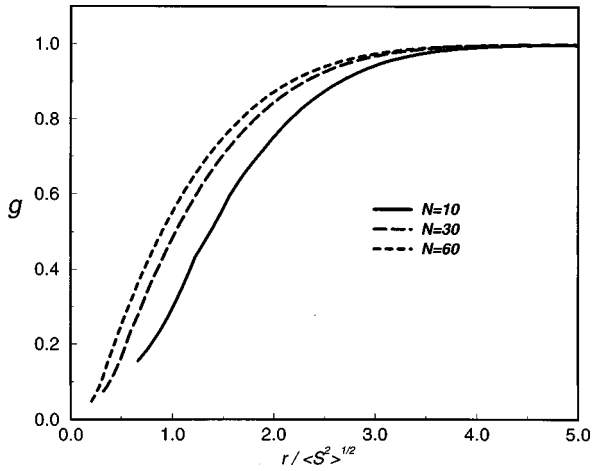

FIG. 2. Average site–site correlation function [as defined by Eq. (18)] at zero density for the pearl-necklace-like model with 10 (solid line), 30 (long dashed line) and 60 (short dashed line) monomer units. The site–site distance r is scaled by the square root of the mean square radius of gyration of the molecule $\langle S^2\rangle^{1/2}$.

(3) At zero density the site–site correlation function reaches an asymptotic form for large values of N when the site–site distance is scaled by the the mean radius of gyration.

We have also obtained the individual $\overline{g_{kl}}$ at zero density for the hard alkane models considered in this work (linear and branched). These site–site correlation functions are needed for the implementation of the mean field perturbation theory of alkanes presented in the following paper. Second virial coefficients and site–site correlation functions of alkanes (linear and branched) obtained in this work will be used for the implementation of this perturbation theory.

V. CONCLUSIONS

In this work we have computed numerically the second virial coefficient for hard models of both linear and branched alkanes. It is found that branching reduces the value of the second virial coefficient when compared to a linear chain with the same number of carbon atoms. When branching occurs in the middle of the chain, this decrease is more pronounced. Furthermore, when branching occurs in a given position, two methyl groups reduces more efficiently the second virial coefficient than an ethyl group. The results of this work show that branching changes substantially the second virial coefficient of hard alkane chains. It is expected that this difference will also be reflected in the equation of state. This expectation is born from the fact that a very good EOS for hard n-alkanes has been recently proposed where the solely knowledge of B_2 was enough to predict the compressibility factor in all the density range. Agreement between this EOS and simulation was very good for linear chains. We expect this to be also true for branched alkanes.

A simple prescription to estimate the crossed virial coefficient was provided and good agreement with the numerical data was found. Virial coefficients for a pearl-necklace-like model were also determined. In this model the bond angle was fixed and only three discrete values were allowed for the torsional angles. A comparison was made with a

model with no restrictions on the bond and torsional angles. Differences between both models were very small.

A methodology based on convex body geometry is proposed to estimate the second virial coefficient of chains. It has been shown that this methodology predicts correctly the second virial coefficients of the different conformers of branched alkanes. For linear chains this was also shown in previous work. The second virial coefficient between different conformers can be also correctly estimated from a simple prescription [i.e., Eq. (6) of this work]. These two facts lead to a quite good estimate of the second virial coefficient of linear and branched alkanes. The method seems to work properly for chains with up to 100 monomer units. For longer chains the methodology fails and the scaling law of the second virial coefficient predicted by this approximate method is not correct.

Finally, some results were presented for the site–site correlation function of the pearl-necklace-like model in the limit of zero density. It is shown that the contact value of the site–site correlation function tends to zero as the length of the chain increases. Also the region where the site–site correlation function is less than one increases with the size of the chain, and it is roughly of the order of several times the mean radius of gyration of the molecule.

The results presented in this work will be used in the perturbation theory of alkanes proposed in the following paper.

ACKNOWLEDGMENTS

We thank Dr. D. N. Theodorou and Dr. L. R. Dodd for sending us their FORTRAN code for the determination of the surface and volume of a polymer molecule. Financial support is due to Project No. PB97-0329 of the Spanish DGICYT (Dirección General de Investigación Científica y Técnica). L.G.M. wishes to thank the University Complutense de Madrid for the award of a predoctoral grant.

APPENDIX A: THE MAYER FUNCTION OF POLYMERS FROM A COLLISION ALGORITHM

The algorithm we use in this work is based on the fact that the history of all the collisions of two conformers at fixed relative orientation as they are moved along the intermolecular center of mass vector, $\mathbf{R_{CM}}$, may be determined by a single evaluation of the interatomic distances. In this way one can reduce the computational cost with respect to traditional methods by as many times as there are nodes in $\mathbf{R_{CM}}$.

Consider two conformers, i and j, whose center of mass is placed at the origin of a laboratory reference frame. Let $\{\mathbf{r_k^0}\}$ and $\{\mathbf{r_l^0}\}$ be the set of initial coordinates of the spheres of conformers i and j, respectively, for a given relative orientation defined by ω_i and ω_j.

Let us now translate the center of mass of conformer j along the z axis, in small steps of length ξ. The coordinates of atoms in this molecule after n steps are simply given by:

$$\mathbf{r_l^n}=\mathbf{r_l^0}+n\xi\hat{k}, \tag{A1}$$

where $\hat{k}$ is a unit vector along the z axis. Subtracting $\mathbf{r_k^0}$ from $\mathbf{r_l^n}$ it may be trivially shown that the condition for overlapping of the spheres is given by:

$$n\xi<\pm(\sigma^2-b_{kl}^2)^{1/2}-\Delta z_{kl}^0, \tag{A2}$$

where

$$\Delta z_{kl}^0=z_l^0-z_k^0,$$

$$b_{kl}^2=(x_l^0-x_k^0)^2+(y_l^0-y_k^0)^2.$$

b_{kl} is the well-known impact parameter of collision theory and the plus and minus sign in the first term of the r.h.s. describe whether the collision occurs at the right or at the left of sphere k, respectively.

Let us now divide all the possible pairs of atoms $\{k,l\}$, into three different categories, depending on the number of roots they have in Eq. (A2):

1. Those pairs that will never collide (no roots), which we may ignore. These pairs are determined from either of two conditions:
   (a) $b_{kl}^2>\sigma^2$,
   (b) $\Delta z_{kl}^0>0$ and $\sigma^2<\Delta z_{kl}^0+b_{kl}^2$.
2. Those pairs that initially overlap (one root), which may be determined from the condition $\sigma^2>\Delta z_{kl}^0+b_{kl}^2$. For each of these pairs we calculate the value of n, h_{kl}, such that overlap no longer occurs.
3. Those pairs that will eventually overlap (two roots), which are determined from the condition $\sigma^2<\Delta z_{kl}^0+b_{kl}^2$ and $\Delta z_{kl}^0<0$. For each of the pairs in this group we calculate, (i) the value of n, m_{kl}, for which overlap will begin to occur and (ii) the value of n, o_{kl}, where overlap will stop occurring.

Once the sets $\{h_{kl}\}$, $\{m_{kl}\}$ and $\{o_{kl}\}$ are determined, the Mayer function for the orientation ω_i,ω_j may be evaluated for all the nodes of R_{CM}, $R_{\mathrm{CM},n}$, by the iterative procedure described below:

1. If $\{h_{kl}\}$ is not an empty set, find its biggest element, h_{ij} and set $f(R_{\mathrm{CM},n})=-1$ as long as $n<h_{ij}$.
2. If $\{h_{kl}\}$ is an empty set,
   (a) find the smallest element of $\{m_{kl}\}$, m_{ij} and set $f(R_{\mathrm{CM},n})=0$ as long as $n<m_{ij}$,
   (b) set $f(R_{\mathrm{CM},n})=-1$ for all n such that $m_{ij}\leqslant n<o_{ij}$.
3. Update the set of $\{h_{kl}\}$ by including those elements of $\{o_{kl}\}$ such that $m_{kl}<n<o_{kl}$. Also, exclude these elements from $\{m_{kl}\}$ and $\{o_{kl}\}$.
4. Repeat the procedure until $\{h_{kl}\}$, $\{m_{kl}\}$ and $\{o_{kl}\}$ become empty sets.

The algorithm described is useful for a system of hard spheres but it may be easily extended to molecules where the interaction site is a hard sphere plus a square well.

APPENDIX B: SCALING LAW OF B_2 AS OBTAINED FROM CONVEX BODY GEOMETRY

In this Appendix we derive the scaling law of B_2 as predicted from the empirical method proposed in Ref. 17 and used in this work.

A look at Eq. (10) shows that B_2 should scale as $\overline{V\alpha}$. On the other hand, Eq. (9) shows that $\overline{\alpha}$ scales as $\overline{RS/V}$, since the second member of the right hand side is a small correction term. Now, one expects that both S and V be linear functions of N, so that, essentially, $\overline{\alpha}$ scales as $\overline{R}$. One is thus lead to the believe that any convex body approach will lead to a scaling law for B_2 of the form:

$$B_2 \propto \overline{V} \cdot \overline{R}. \tag{B1}$$

In the approach proposed in Ref. 17, the value of R for a given conformer is taken to be that of a parallelepiped with sides chosen such that its principal moments of inertia match those of the conformer. Using Eqs. (23)–(26) of Ref. 17 it can be shown that this leads to the following expression for R:

$$R = \sqrt{\frac{3}{8N}} \left(\sqrt{I_x + I_y - I_z} + \sqrt{I_x + I_z - I_y} + \sqrt{I_y + I_z - I_x} \right), \tag{B2}$$

where I_x, I_y and I_z stand for the three principal moments of inertia of the conformer.

Now, both theoretical considerations[43] and numerical calculations[20] show that as N goes to infinity, the ratio of the principal moments of inertia of a flexible molecule reaches a constant, well defined value. This implies that each of the square roots of Eq. (B2) scale in the same way and we need consider just one of them in order to study the scaling behavior of R. Using Eq. (27) of Ref. 17 for the principal moments of inertia, and considering only the first square root of Eq. (B2), one gets:

$$R \propto \sqrt{\frac{1}{N} \sum_{k=1}^{N} z_k^2}. \tag{B3}$$

In terms of the mean radius of gyration, this scaling behavior may be written as:

$$R \propto \sqrt{S^2}. \tag{B4}$$

So that one expects that $\overline{R}$ will scale as $\langle S^2 \rangle^{1/2}$. This leads to the following scaling behavior for B_2:

$$B_2 \propto N \langle S^2 \rangle^{1/2} \propto N^{1+\nu} \propto N^{1.588}. \tag{B5}$$

Actually, Eq. (B1) shows that any convex body approach with a mean radius of curvature scaling as the mean radius of gyration will lead to a wrong scaling behavior for B_2.

APPENDIX C: CALCULATION OF THE SITE–SITE CORRELATION FUNCTIONS

Let us start computing the site–site correlation function between two molecules of fixed geometry. Later, we shall show how to perform the average over all pairs of conformers. The site–site correlation function, g_{kl}^{ij}, between site k of molecule i and site l of molecule j (where i and j may be for instance two different conformers), can be obtained from the pair correlation function of the molecules by the following equation:

$$g_{kl}^{ij}(r) = \int g_2(R_{\mathrm{ref}}, \omega_i, \omega_j) p_{kl}(R_{\mathrm{ref}}, \omega_i, \omega_j; r) \times \frac{R_{\mathrm{ref}}^2}{r^2} \frac{dR_{\mathrm{ref}}}{dr} d\omega_i d\omega_j, \tag{C1}$$

where R_{ref} is the distance between the reference points (one in molecule i and the other in molecule j) which define the position of the molecules while ω_i and ω_j are vectors defining their orientation; g_2 is the molecular pair correlation function and p_{kl} is the fraction of molecules found in an infinitesimal interval around $(R_{\mathrm{ref}}, \omega_i, \omega_j)$, such that the distance between sites i and j lye in the interval $[r+dr]$. This equation may be derived by equating the number of molecules with sites k,l at a distance r as obtained from the definitions of g_{kl}^{ij} and g_2.

Equation (C1) can be implemented numerically in two different ways depending on the choice of the reference point used to define the location of the molecule. Usually, the center of mass is the choice. In this case, R_{ref} is just the distance between the centers of mass of the molecules, i.e., R_{CM} (Method 1). However, another possible choice is to use site k as the reference point of molecule i and site l as the reference point of molecule j (Method 2). Let us describe briefly the implementation of both methods:

Method 1. We divide the distance between the center of mass, R_{CM}, in M small intervals of size ΔR_{CM} and use a simple trapezoid rule to integrate over R_{CM} for each different orientation. Mathematically, we express this as:

$$g_{kl}^{ij}(r) = \sum_{n=1}^{M} \left\langle g_2(R_{\mathrm{CM},n}, \omega_i, \omega_j) p_{kl}(R_{\mathrm{CM},n}, \omega_i, \omega_j; r) \frac{R_{\mathrm{CM},n}^2}{r^2} \right\rangle, \tag{C2}$$

where the brackets denote an orientational average. This orientational average is performed with N_{ori} relative orientations. In Eq. (C2) the index n runs over the M values of R_{CM}. Since we are considering the zero density limit, g_2 is either null or unity, depending on whether there is overlap between the molecules or not, while p_{kl} takes the value of 1 if sites k and l are found in the interval $[r, r+\Delta R_{\mathrm{CM}}]$ and zero otherwise. This choice for p_{kl} ensures that the ratio of dR to dr that appears in Eq. (C1) becomes unity. An expression which differs from Eq. (C2) only in the quadrature rule was proposed for the first time by Alvarez *et al.*[44] and by Anta.[45]

Method 2. In this case R_{ref} is just r and p_{kl} is obviously equal to one. Accordingly, Eq. (C1) can be rewritten as:

$$g_{kl}^{ij}(r) = \langle g_2(r, \omega_i, \omega_j) \rangle. \tag{C3}$$

It is straightforward to show that the average of the r.h.s. of the above equation is related to the Mayer function, as measured from reference points at k and l. Thus, in order to calculate $g_{kl}^{ij}(r)$ one can just as well use the efficient algorithm described in Appendix A. This alternative may turn out to be quite convenient if the number of monomers of the molecule is small.

To check both methods we computed the zero density limit of the site–site correlation functions for the simple hard dumbbell system. Results obtained from Eq. (C2) were identical to those of Eq. (C3) and moreover we got perfect agreement with previously published results for this system.[46]

Once the site–site correlation function between sites k and l has been obtained for a pair of molecules of fixed geometry there is still the problem of obtaining the conformational average, according to the following equation:

$$\overline{g_{kl}}=\sum_{i=1}^{i=q}\sum_{j=1}^{j=q}x_i x_j g_{kl}^{ij}. \tag{C4}$$

This average was solved numerically by means of a MC sampling procedure, equal to that described in the text for the second virial coefficients.

[1] J. P. Ryckaert and A. Bellemans, Chem. Soc. Faraday Discuss. **66**, 95 (1978).
[2] N. G. Almarza, E. Enciso, J. Alonso, F. J. Bermejo, and M. Alvarez, Mol. Phys. **70**, 485 (1990).
[3] D. Brown, J. H. R. Clarke, M. Okuda, and T. Yamazaki, J. Chem. Phys. **100**, 1684 (1994).
[4] P. Padilla and S. Toxvaerd, J. Chem. Phys. **94**, 5650 (1991).
[5] J. Gao and J. H. Weiner, J. Chem. Phys. **91**, 3168 (1989).
[6] R. Dickman and C. K. Hall, J. Chem. Phys. **89**, 3168 (1988).
[7] B. Smit, S. Karaborni, and J. I. Siepmann, J. Chem. Phys. **102**, 2126 (1995).
[8] A. D. Mackie, A. Z. Panagiotopoulos, and S. Kumar, J. Chem. Phys. **102**, 1014 (1995).
[9] J. G. Curro and K. S. Schweizer, Adv. Chem. Phys. **98**, 1 (1997).
[10] K. G. Honnell and C. K. Hall, J. Chem. Phys. **90**, 1841 (1989).
[11] E. Kierlik and M. L. Rosinberg, J. Chem. Phys. **97**, 9222 (1992).
[12] M. S. Wertheim, J. Chem. Phys. **87**, 7323 (1987).
[13] W. G. Chapman, G. Jackson, and K. E. Gubbins, Mol. Phys. **65**, 1057 (1988).
[14] T. Boublik, C. Vega, and M. D. Peña, J. Chem. Phys. **93**, 730 (1990).
[15] A. Yethiraj, K. G. Honnell, and C. K. Hall, Macromolecules **25**, 3979 (1992).
[16] P. Padilla and C. Vega, Mol. Phys. **84**, 435 (1995).
[17] C. Vega, L. G. MacDowell, and P. Padilla, J. Chem. Phys. **104**, 701 (1996).
[18] C. Vega, S. Lago, and B. Garzon, J. Chem. Phys. **100**, 2182 (1994).
[19] P. J. Flory, *Statistical Mechanics of Chain Molecules* (Wiley, New York, 1969).
[20] C. Vega and A. L. Rodriguez, J. Chem. Phys. **105**, 4223 (1996).
[21] In Ref. 20, there was a misprint in the value used for E_2. We actually used 2700 cal/mol and not the reported value of 2000 cal/mol.
[22] H. Conroy, J. Chem. Phys. **47**, 5307 (1967).
[23] I. Nezbeda, J. Kolafa, and S. Labik, Czech. J. Phys., Sect. B **39**, 65 (1989).
[24] M. P. Allen and D. J. Tildesley, *Computer Simulation of Liquids* (Clarendon, Oxford, 1987).
[25] N. Madras and A. D. Sokal, J. Stat. Phys. **50**, 109 (1988).
[26] H. Hadwiger, *Altes und Neues uber konvexe Korper* (Birkhauser, Basel, 1955).
[27] T. Kihara, Adv. Chem. Phys. **5**, 147 (1963).
[28] T. Boublik and I. Nezbeda, Collect. Czech. Chem. Commun. **51**, 2301 (1986).
[29] E. Enciso, J. Alonso, N. G. Almarza, and F. J. Bermejo, J. Chem. Phys. **90**, 413 (1989).
[30] M. Rigby, Mol. Phys. **32**, 575 (1976).
[31] L. R. Dodd and D. N. Theodorou, Mol. Phys. **72**, 1313 (1991).
[32] J. Alejandre, S. E. Martinez-Casas, and G. A. Chapela, Mol. Phys. **65**, 1185 (1988).
[33] J. Dautenhahn and C. K. Hall, Macromolecules **27**, 5399 (1994).
[34] P. J. Flory, *Principles of Polymer Chemistry* (Cornell University Press, Ithaca, 1953).
[35] H. Fujita, Macromolecules **21**, 179 (1988).
[36] A. M. Rubio and J. J. Freire, Macromolecules **29**, 6946 (1996).
[37] J. J. Freire, A. M. Rubio, and A. Poncela, Macromol. Symp. **121**, 97 (1997).
[38] W. Bruns, Macromolecules **29**, 2641 (1996).
[39] P. G. de Gennes, *Scaling Concepts in Polymer Physics* (Cornell University Press, Ithaca, NY, 1979).
[40] K. F. Freed, *Renormalization Group Theory of Macromolecules* (Wiley, New York, 1987).
[41] B. Li, N. Madras, and A. Sokal, J. Stat. Phys. **80**, 661 (1995).
[42] G. S. Singh and B. Kumar, J. Chem. Phys. **105**, 2429 (1996).
[43] K. Solc, J. Chem. Phys. **55**, 335 (1971).
[44] M. Alvarez, E. Lomba, C. Martin, and M. Lombardero, J. Chem. Phys. **103**, 3680 (1995).
[45] J. A. Anta, Ph.D. thesis, Universidad Complutense de Madrid, 1997.
[46] L. L. Lee, *Molecular Thermodynamics of Nonideal Fluids* (Butterworth, Boston, 1988).